EC Contract SES6-CT-2003-502706

PARTICIPANT ORGANIZATION NAME: UMR CNRS ULP 7516

Related with Work Package…….

Related with Working Group…….

EFFECTS OF THE ROUGHNESS OF A FRACTURE ON THERMAL EXCHANGE

Amélie Neuville, Renaud Toussaint, Jean Schmittbuhl
**Institut de Physique du Globe de Strasbourg, UMR CNRS ULP 7516*
EOST, Université Louis Pasteur, 5 Rue René Descartes, 67084 Strasbourg, France
e-mail: amelie.neuville@eost.u-strasbg.fr
(Draft Version)

ABSTRACT

Heat exchange during laminar flow in an open fracture is studied numerically on the basis of the Stokes equation in the limit of hydro-thermal lubrication. We study the influence of fracture roughness on hydraulic permeability and heat flux through the fracture sides when a cold fluid is injected into a homogeneous hot host rock. As a first step, the temperature rock is supposed to be constant so that we only deal with the spatial temperature evolution inside the fluid. We use realistic aperture geometry and parameters to illustrate our modeling. Then we show a simplified thermal simulation by using only little spatial information about the hydraulic flow.

INTRODUCTION

The modeling of the fluid transport in low permeable crustal rocks is of central importance for many applications (Neuman, 2005). Among them is the monitoring of the geothermal circulation in the project of Soulz-sous-Forêts, France (Bachler et al, 2003), where the heat exchange especially occurs through open fractures in granite (Gérard et al., 2006).
Numerous hydro-thermal simulations have already been proposed: some analytical solutions are known for simple geometry like parallel plates (e.g. Turcotte & Schubert, 2002), flat circular cylinders (Heuer et al., 1991). It exists as well more complex models, for instance: modeling occurring through a tridimensional network of fractures organized according to geological observations eventually added with stochastical fractures (like in Soultz-sous-Forêts, France, e.g. Gentier et al., 2006; Rachez et al., 2007 or in Rosemanowes, U.K., Kolditz & Clauser, 1998). Nevertheless, the geometry of each fracture itself is simple and in Kolditz and Clauser, 1998 it is suspected that some differences between the heat model and what is observed could be due to fracture channeling from roughness and network channeling. Channeling of the fluid flow has indeed already been experimentally observed (e.g Méheust & Schmittbuhl, 2000; Plouraboué et al., 2000) within rough fracture.
Here, we focus on the fracture scale, and the specificity of our hydro thermal model is to take into account the different scale variations of the fracture morphology. We aim at bringing out the main parameters which change the hydraulic and thermal behavior and quantifying the results. The further idea would be to take into account the roughness in network model by simply correcting macroscopic parameters.
We first describe our model of fracture thanks to self-affine apertures. Then, using lubrication approximations, we obtain bidimensional (2D) pressure and thermal equations when a cold fluid is injected through a fracture in a stationary regime. The temperature within the surrounding rock is supposed to be hot and constant (in time and space), with the fluid density being constant. We assume that at a coarse grained scale, the one dimensional (1D) basic equation for heat flux is identical to the one for parallel plates, but with a suitable characteristic thermal length which is different from the one computed with the mechanical aperture.
The numerical hydraulic and thermal results are illustrated for a given fracture morphology by trying to use realistic parameters (roughly inspired by the one of Soultz-sous-Forêts). Then we aim at bringing out what hydraulic information we need to have an idea of the thermal field. Thus we roughly estimate the temperature field by using only restricted spatial information about the hydraulic field (here obtained thanks to spatial Fourier filtering).

MODELING

Roughness of the fracture aperture

It has been shown that a possible geometrical model of rough fractures consists in using self affine surfaces, statistically invariant upon an isotropic scaling within their mean plane while on the perpendicular direction, the scaling is anisotropic (e.g. Brown & Scholz, 1985, Power et al., 1987; Cox & Wang, 1993; Schmittbuhl et al, 1993; Schmittbuhl et al 1995). To simplify the notation, we consider that the mean fracture plane (Figure 1) is described by the $(\hat{x},\hat{z})$ coordinates and perpendicular direction is $\hat{y}$. Such a self affine surface is invariant under the scaling transformation $x \rightarrow \lambda x$, $z \rightarrow \lambda z$ and $y \rightarrow \lambda^{\zeta} y$, where ζ is called the roughness exponent or Hurst exponent. Many rock surfaces exhibit a Hurst exponent equal to $\zeta = 0.8$ (granite, etc) (Bouchaud, 1997, Schmittbuhl et al, 1993, Schmittbuhl et al, 1995; Santucci et al., 2007) or to $\zeta = 0.5$ (sandstone) (Boffa et al., 1998; Méheust, 2002).
It is important to note that a self-affine surface having a roughness exponent inferior to 1 is asymptotically flat at large scales (Roux et al., 1993). Accordingly, the self-affine topography can be seen as a perturbation of a flat interface. Due to the lubrication approximation (Pinkus & Sternlich, 1961), which holds with smooth enough self affine perturbations, we will see that only the local aperture controls the problem. Therefore, the only input is the aperture field (also called geometrical aperture). The difference between two uncorrelated self-affine fracture sides having the same roughness exponent is as well a self-affine function (Méheust & Schmittbuhl, 2003). Thus we generate numerical apertures by using self-affine functions.
Several independent self-affine aperture morphologies are generated with the same roughness exponent chosen equal to $\zeta = 0.8$. They exhibit various pattern morphologies, various root-mean square deviations (RMS, denoted as σ), mean geometrical apertures A and size (length l_x and height l_z). The local aperture can be expressed as $a(x,z) = A + \sigma.a'(x,z)$, where A is the spatial average of a,

$\sigma = \left(\iint a^2 dxdz\right) / \left(l_x \cdot l_z\right) - A^2$ and a' is a self-affine perturbation having ζ as exponent, with a spatial average being null and a RMS equal to one. To keep simple boundary geometry of the domain where the equations are solved (i.e. where the aperture is not null), we do not allow any contact area by probing a range of strictly positive normalized aperture fields.
It has to be noticed that our hydro-thermal model can be applied to other variable aperture which might be more relevant depending on the geological context.

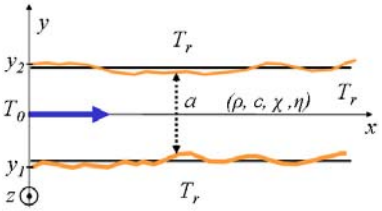

Figure 1: Schematic fracture with variable aperture a(x,z); ρ, c, χ, η *are respectively the following fluid properties: density, heat capacity, thermal diffusivity and dynamic viscosity.*

Hydraulic flow

The hydraulic flow is obtained under the same hypotheses and solved in the same way as in Méheust & Schmittbuhl, 2001: we use finite differences, and the system of linear equations is inverted using an iterative biconjugate gradient method (Press et al., 1992).
We impose the pressure drop across the system, and study the steady state flow of a Newtonian fluid at low Reynolds number, so that the viscous term of the Navier-Stokes dominates the inertial one (Stokes, 1856; Batchelor, 1967): $\vec{\nabla} P = \eta \Delta \vec{v}$, where η is the dynamic viscosity, $\vec{v}$ the velocity of the fluid and P is the pressure deviation from the hydrostatic profile (or the hydraulic head, equal to the pressure corrected by the gravity effect). To be in the framework of the lubrication approximation (Pinkus & Sternlich, 1961), besides small Reynolds number, we consider fractures with flat enough sides. Therefore, the velocity vectors get negligible components normal to the mean fracture. We consider that a macroscopic forced pressure gradient imposed along the $\hat{x}$ axis; $\hat{y}$ is denoted as the axis perpendicular to the mean fracture plane, and $\hat{z}$ is the in plane unit vector perpendicular to the mean flow direction. This leads us to express the velocity as a parabolic law (e.g. Iwai, 1976) (Figure 2):

$$\vec{v}(x,y) = \frac{\vec{\nabla}_2 P}{2\eta}(y - y_1)(y - y_2) \quad \text{[Eq. 1],}$$

where y_1 and y_2 are the fracture sides coordinates and $\vec{\nabla}_2$ is the gradient operator in the fracture plane. The hydraulic flow through the fracture aperture is (cubic law):

$$\vec{q}(x,z) = \int_a v(x,y,z)dy = -\frac{a^3}{12\eta}\vec{\nabla}_2 P \quad \text{[Eq. 2],}$$

and the bidimensional (2D) velocity is defined from the average of the velocity over the aperture with

$$\vec{u}(x,z) = -\frac{a^2}{12\eta}\vec{\nabla}_2 P \quad \text{[Eq 3].}$$

Furthermore, considering the fluid to be incompressible, the Reynolds equation is obtained: $\vec{\nabla}_2(a^3 \vec{\nabla}_2 P) = 0$. As boundary conditions of this equation, we impose the pressure at the inlet and outlet of the fracture (if $x = 0$, $P = P_0$ and if $x = l_x$, $P = P_L$, with $P_0 > P_L$) and consider impermeable sides at $z = 0$ and $z = l_z$.

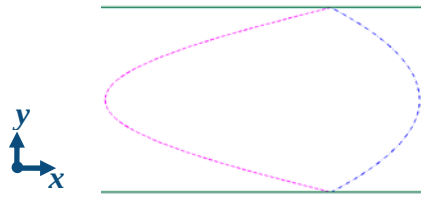

Figure 2: Velocity quadratic profile (dashed line) and temperature quartic profile (dot-dashed line) inside a fracture along the aperture; arbitrary abscissa units. Along the fracture sides, v=0 *and* T=T_r, *and the roots of the polynoms given by equations 1 and 4 are respected.*

Thermal exchange

On the basis of a classical description (e.g. Turcotte & Schubert, 2002), we aim at modeling the fluid temperature when cold water is permanently injected at the inlet of the hot fracture at temperature T_0. As the conduction inside the rock is not taken into account (hypothesis of infinity thermal conduction inside the bedrock), the fracture sides are supposed to be permanently hot at the fixed temperature T_r. This hypothesis should hold for moderate time scales (e.g., months), after the fluid injection has stabilized, and before the rock temperature has significantly changed. The fluid temperature is controlled by the balance between thermal convection and conduction inside the fluid, which reads (Landau & Lifchitz, 1994): $\vec{v} \cdot \vec{\nabla} T = \chi \Delta T$ where χ is the thermal diffusivity of the fluid and T the fluid temperature. We extend the lubrication approximation by considering that the slopes of the fracture morphology are small enough to provide conduction oriented along y axis. We suppose that the leading terms are conduction along y axis and in plane convection (no velocity component along $\hat{y}$); the vertical free convection (order of magnitude is km/year from Bataillé et al, 2006) as well as the fluid conduction along $\hat{x}$ and $\hat{z}$ axes are neglected, so that the previous equation is reduced to :

$$\frac{\partial^2 T}{\partial y^2} = \frac{v_x}{\chi}\frac{\partial T}{\partial x} + \frac{v_z}{\chi}\frac{\partial T}{\partial z} \quad \text{[Eq. 4].}$$

The fluid temperature is supposed to be the one of the rock along the fracture sides, and the fluid is supposed to reach the temperature rock at a long enough distance. When we integrate this quantity along the fracture aperture we assume that $\beta = q_x \frac{\partial T}{\partial x} + q_z \frac{\partial T}{\partial z}$ is mainly dependent on (x,z) (few dependence on z if we are away from the fracture sides), where q_x and q_z are the x and z component of $\vec{q}$ defined in Eq. 2. In this way, we find that the temperature solution has a quartic profile (Figure 2) along the fracture aperture [1]:

$$T = -\frac{\beta}{2a^3\chi}(y - y_1)(y - y_2)(y - \sqrt{5}y_1)(y - \sqrt{5}y_2) + T_r \quad \text{[Eq.5],}$$

where y_1 and y_2 are the fracture sides coordinates.

[1] We develop as well another kind of algorithm based on Lattice Boltzmann method, which requires very few hypotheses, in order to solve the velocity and temperature fields. From those results it appears that the respective parabolic and quartic solutions (with the proper coefficients) are indeed right more or less 5%.

Similarly to what we do for the hydraulic flow, we solve the thermal equation by integrating it along the fracture aperture (consequence of the lubrication approximation extended for the thermal aspect). In particularly, when doing the balance of the energy flux, we express the advected free energy flux as $\vec{\nabla}_2\left(\rho c\int_a v(x,y,z)[T(x,y,z)-T_0]dy\right)$. Consistently with this energy budget, we introduce the relevant quantity $\overline{T}$ which is an average temperature weighted by the velocity:

$$\overline{T}(x,z)=\frac{\int_a v(x,y,z)T(x,y,z)dy}{\int_a v(x,y,z)dy} \quad \text{[Eq. 6].}$$

We also use the Nusselt number $Nu=-\varphi_r/\varphi_{ref}$ which compares the efficiency of the present heat flow at the fracture side $\varphi_r=-\chi\rho c\left.\frac{\partial T}{\partial y}\right|_{y=z_1,z_2}$ and the mesoscopic flow at the fracture aperture scale without convection: $\varphi_{ref}=\chi\rho c\left(T_r-\overline{T}\right)/a$. Using the polynomial expression of T (Eq. 5) and $\overline{T}$ definition, we get $Nu=\frac{70}{17}$. Rearranging the simplified equation of thermal convection and conduction balance (Eq. 4), we get the final equation to be solved:

$$\vec{q}\cdot\vec{\nabla}_2\overline{T}+2\frac{\chi}{a}Nu\left(\overline{T}-T_r\right)=0 \quad \text{[Eq. 7],}$$

with boundary conditions $\overline{T}(0,z)=T_0$ at the inlet and $\overline{T}(z)\xrightarrow{x\to\infty}T_r$ at the outlet. Moreover any boundary condition can be used along $z=0$ or $z=l_z$, as the hydraulic flow is null there.
We discretize this equation by using a first order finite differences scheme and finally get $\overline{T}$ by inversing the system using a conjugated gradient method (Press et al., 1992).

Characterization of the computed hydraulic and thermal fields

Comparison to modeling without roughness

If we consider a fracture modeled with two parallel plates separated by a constant aperture A, then the gradient of pressure is constant all along the fracture as well as the hydraulic flow which is equal to:

$\vec{q}_{//}=-\frac{\Delta P}{l_x}\frac{A^3}{12\eta}\hat{x}$, where the subscript // denotes results valid for parallel plates and $\Delta P = P_L - P_0$. Under these conditions the analytical solution of Eq. 7 for parallel plates is:

$$\overline{T}_{//}=(T_0-T_r)\,exp\left(-\frac{x}{R_{//}}\right)+T_r \quad \text{[Eq. 8],}$$

where $R_{//}$ is a thermal length describing the distance at which the fluid reaches the temperature of the surrounding rock. It is defined by:

$$R_{//}=\frac{A\left\|\vec{q}_{//}\right\|}{2Nu\,\chi}=-\frac{\Delta P}{l_x}\frac{A^4}{24\eta Nu\,\chi}=\frac{APe}{Nu} \quad \text{[Eq. 9],}$$

where Pe is the Peclet number defined by $Pe=\left\|\vec{q}_{//}\right\|/2\chi$. Pe expresses the convection importance compared to the conduction. For rough fractures, we want to study whether the temperature profiles can still be described by Eqs. 7 and 8 at a coarse grained case. If this is the case within some approximation, the goal of our study becomes to understand how the roughness affects the thermalization, and more precisely to quantify the suitable thermalization length R: when the modeled temperature profile is fitted by an exponential profile similar to Eq. 8, we obtain a suitable thermal length R that depends on the fracture morphology.

Hydraulic aperture

The hydraulic flow can be macroscopically quantified with the hydraulic aperture H (Brown, 1987; Zimmerman, 1991), defined as the equivalent parallel plate aperture to get the macroscopic flow $\langle q_x\rangle$ under the pressure gradient $\Delta P/l_x$:

$$H=\left\langle -q_x\frac{12\,\eta\,l_x}{\Delta P}\right\rangle^{1/3} \quad \text{[Eq. 10],}$$

where the quantity under bracket like $\langle q_x\rangle$ is the spatial average of what is inside the brackets. On the field this H value is probably a quantity which can be determined by hydraulic tests while A is the value we get an idea of using optical or geometrical measurements. If H/A is higher than 1, then the fracture is more permeable than parallel plates separated by $a(x, y) = A$. As the hydraulic aperture can be inhomogeneous, we define as well a local hydraulic aperture with:

$$h(x,z)=\left(-q_x(x,z)\frac{12\eta l_x}{\Delta P}\right)^{1/3} \quad \text{[Eq. 11].}$$

Local quantities (geometrical and hydraulic apertures) are denoted with small letters and macroscopic variables (mean geometrical and hydraulic aperture) are in capital letters.

Thermal length

For the thermal aspect, once $\overline{T}$ is known, we aim at defining a thermal length R. To do that, we first define $\overline{\overline{T}}$, a 1D temperature which varies in the forced gradient direction, fulfilling the energy conservation:

$$\overline{\overline{T}}(x)=\frac{\int_a u_x(x,z)\overline{T}(x,z)dz}{\int_a u_x(x,z)dz} \quad \text{[Eq. 12].}$$

It is the average of $\overline{T}$ along the width of the fracture l_z, weighted by u_x which is the x component of the 2D velocity (defined in Eq. 3).

Then, based on the flat plate temperature solution (Eq. 8), we do a linear regression of $ln\left[\left(\overline{\overline{T}}-T_r\right)/\left(T_0-T_r\right)\right]$ plotted as a function of x, and we use the slope of this model line to get the characteristic thermal length R. The regression is computed with least square minimization for abscissa from $x=0$ to the minimum x value so that $\left|\frac{\overline{\overline{T}}-T_r}{T_0-T_r}\right|<2\cdot10^{-6}$.

This thermal length can be linked to a "thermal aperture" Γ by using a similar definition to the one given in Eq. 9 :

$$R=-\frac{\Delta P}{l_x}\frac{\Gamma^4}{24\eta Nu\,\chi}$$

It means that parallel plates separated by the proper aperture Γ will provide the same averaged thermal behavior as the rough plates.

APPLICATION

Example of computed hydro-thermal fields

Let us consider the wells GPK3 and GPK2 near Soultz-sous-Forêts, which are separated by a distance of about 600m at about 5000 m of depth. From hydraulic tests (Sanjuan et al., 2006), it has been shown that the hydraulic connection is relatively direct between both wells: (Sausse et al., 2008) a fault zone consisting on clusters of small fractures would link GPK3 (interception at 4775m) and GPK2. That probably leads to complex hydraulic streamlines and heat exchanges. We study a simplified case with one single fracture and roughly straight streamlines between both wells (linear flow). Then we use parameters (geometrical aperture and pressure gradient) which are probably slightly different from the ones observed or used in practice at Soultz-sous-Forêts.
Figure 3 shows an example of self-affine aperture, randomly generated and dimensioned so that the mean aperture A is equal to $3.60\ mm$ and its standard deviation is $\sigma = 1.23\ mm$.

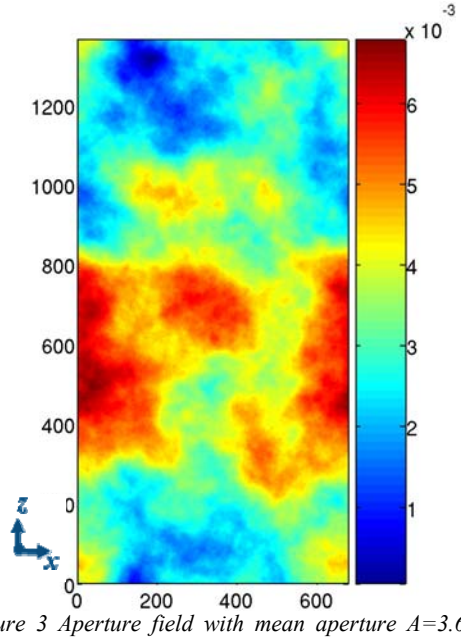

Figure 3 Aperture field with mean aperture A=3.60 mm and variability of the aperture σ=1.23 mm (σ/A=0.34). The color bar represents the aperture in m, the side units are plane spatial coordinates (x,z), also in m.

Then we solve the hydraulic flow in this variable morphology and obtain the 2D velocity field u (Figure 4 shows norm of u, defined in Eq.3) by dimensioning it with $\Delta P/l_x = -10^{-2} bar/m$, which corresponds to about $6\ bars$ between the bottom of both wells. The dynamic viscosity is chosen equal to $4 \times 10^{-4}\ Pa/s$ (reference value for pure water at $10\ Pa$ and $100°C$ from table in Spurk & Aksel, 2008). The size of the studied fracture is l_x x $l_y = 683.3 \times 1366.5$ and using the parallel plate model separated by A, the 2D-velocity expected from the quadratic law is 3.6 m/s and the thermal length is $R_{//} = 33.3m$. As we see, the 2D velocity field exhibits quite high contrasts: the fluid is rather immobile at the upper and lower borders of the fracture (close to $z=0$ and $z=l_x$) while most of the fluid flows very quickly through a channel in the middle of the fracture.
The macroscopic hydraulic aperture is $3.73\ mm$, which is slightly higher than the mean mechanical aperture A. Therefore, this whole fracture is more permeable than parallel plates separated by A. That means as well that this fracture is mechanically thinner than what we would expect from the knowledge of H. However, if the measurement of the hydraulic aperture is local (see in Figure 5), then h ranges from nearly 0 to $5.43\ mm$.

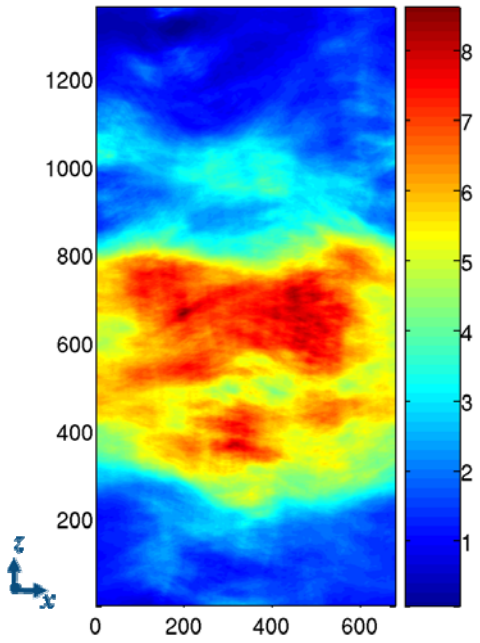

Figure 4: Color map of the velocity field in m/s. Red areas correspond to very high velocity while dark blue areas show static fluid. A linear pressure gradient is imposed between the left and right of the fracture. Spatial coordinates are in m.

It has to be noticed that many individual fracture apertures observed in Soultz are rather thinner ($0.2\ mm$) (Genter & Jung, private communication) while the fracture zone is rather thicker (10cm) (Sausse et al., 2008) and that the pressure gradient is probably higher than what is applied here – however the friction along the well itself may diminishes the pressure difference applied at the well head–. In our simulation, we have to work with small enough velocities (moderate Reynolds number) and we need to fix the pre-supposed macroscopic ratio between convection and conduction (thermal Peclet number). We quantify it indirectly thanks to the ratio $l_x/R_{//}$. $R_{//}$, defined in Eq. 9, is the characteristic thermal length depending on the average aperture, pressure gradient and fluid parameters which can be computed without knowing the exact morphology. All the results we present are still valid under any dimensioning which keeps $l_x / R_{//}$ constant (here equal to 20.5): for instance another dimensioning for other purpose could be $l_x = 691m$, $A = 10mm$ and $\Delta P/l_x = -1.7 \times 10^{-4} bar/m$ (using the same fluid parameters).
The wells does not inject/pump water all along the fracture height (straight streamlines are only an approximation) and the fracture zone between GPK2 and GPK3 is not vertical. The flowrate observed at Soultz is about $Q = 20L/s$, which is probably carried by several fractures. Thus, using a velocity of about $u = 5m/s$ and a fracture aperture equal to $5mm$ means that the well crosses such fractures over a cumulated length of about (by neglecting the well radius):

$$L = \frac{Q}{VA} = \frac{20 \times 10^{-3}}{5 \times 5 \times 10^{-3}} \approx 80cm\,.$$

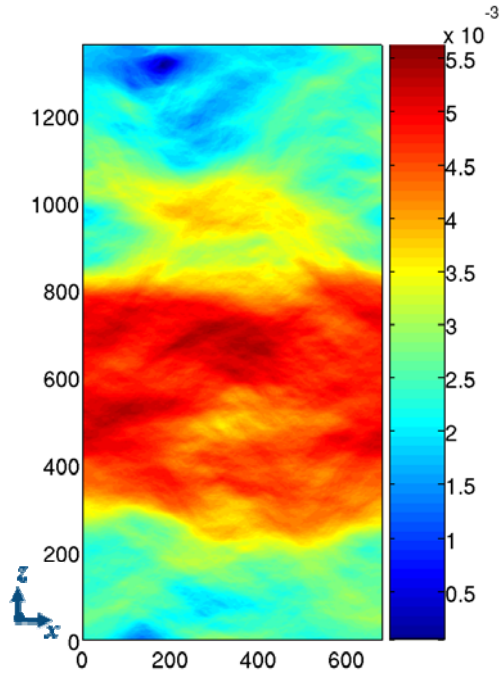

Figure 5: Color map of the local hydraulic aperture in m computed from the variable hydraulic flow and aperture. Spatial coordinates are in m.

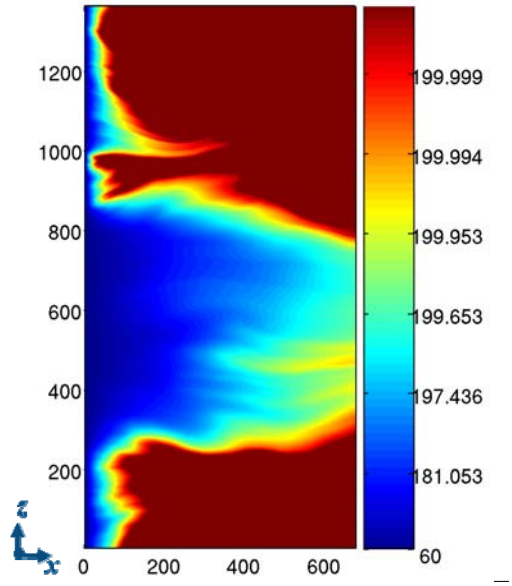

Figure 6: Map of the averaged temperature field $\overline{T}$ in Celsius degrees (°C). The color bar changes exponentially; thus small variations slightly below the temperature rock (200°C) are highly visible. Spatial coordinates are in m.

Figure 6 shows the temperature field $\overline{T}$ computed inside the variable aperture using the variable hydraulic flow. As we see, $\overline{T}$ is very inhomogeneous and exhibits channeling.
The chosen inlet temperature is $T_0=60°C$, the rock temperature is $T_r=200°C$ and the fluid diffusivity is $\chi=0.17mm^2/s$ (water reference value at $T=100°$, from table in Taine & al., 2003). In practice, the rock temperature will evolve because the rock thermal diffusivity is about $1mm^2/s$, while we considerer it as far larger compared to the fluid one (so that T_r is kept constant). Using these parameters we see that the pumping well located at $600m$ within the illustrated fracture geometry is far enough to get hot water.

However, $\overline{T}$ is rather different from what we expect from parallel plates, especially because this field is not at all invariant along $\hat{z}$. That is quantitatively well illustrated in Figure 7 where we plot some profiles of temperature along x for $z=970m$ (plot iv) and $z=703m$ (plot v). For example, at $x=200m$, the fluid is $200°C$ hot in $z=970m$, while in $z=703m$ the temperature is only $183°C$. Let us compare these 1D temperature profiles along x to the one obtained inside parallel plates separated by the aperture A which reads:

$$\overline{\overline{T}}_{//} = (T_0 - T_r)\,exp\left(-\frac{x}{R_{//}}\right) + T_r \quad \text{[Eq. 13].}$$

Following this model (plot iii) the fluid should be as well at $200°C$ in $x=200m$. If we compare $\overline{\overline{T}}_{//}$ to the averaged observed temperature $\overline{\overline{T}}$ (defined in Eq. 12) (Figure 7, plot i), we see that $\overline{\overline{T}}_{//}$ is not well representative. Therefore, we model $\overline{\overline{T}}$ by using an adapted parallel law $\overline{\overline{T}}_{mod}$ (plot ii) which is an exponential law with a suitable thermal length R:

$$\overline{\overline{T}}_{mod} = (T_0 - T_r)\,exp\left(-\frac{x - x_0}{R}\right) + T_r \quad \text{[Eq. 14],}$$

where $R=96.6m$ (i.e. $2.9 \times R_{//}$) and $x_0=9.8m$. Due to the choice of the minimization to obtain parameters R and x_0 (least square applied on the semi-log plot), the beginning of the fit curve is not accurate. The thermal aperture is therefore equal to $\Gamma=4.7\ mm$, which is rather different from the geometrical aperture $A=3.6\ mm$. A larger thermal aperture (compared to the geometrical one) means an inhibited thermalization on average.

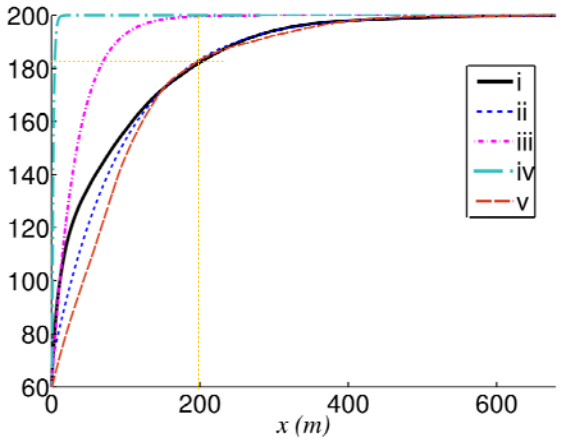

Figure 7 Fluid 1D temperature in °C in function of x. The continuous black curve (i) shows the computed temperature $\overline{\overline{T}}$. The blue dashed curve (ii) is the model of curve (i) with an exponential function. The dot dashed magenta curve (iii) is the fluid 1D temperature by neglecting the self-affinity perturbation (inside flat parallel plates). The curves (iv) and (v) are profiles of temperature $\overline{T}(x,z)$ for respectively z=970m and z=703m.

Temperature estimation with few parameters

The spatial correlation of the hydraulic aperture seems to be a key parameter to evaluate the temperature field. The macroscopic hydraulic aperture H brings too few information

to characterize the heat exchange, while it is quite useless to know in detail the spatially variable hydraulic aperture h (which is by the way impossible on the field). Therefore we propose to characterize the hydraulic aperture with only the largest spatial variations. Numerically, it is possible to obtain them by filtering the hydraulic field in Fourier domain with the following criterion: only the Fourier coefficients so that $\left(\frac{k_x}{2\pi} l_x\right)^2 + \left(\frac{k_z}{2\pi} l_z\right)^2 < 2^2$ are kept, where k_x and k_y are the coordinates of the wave number. Considering that the Fourier transform is discrete, it means that only the average and the first Fourier modes along x and z are left. The hydraulic aperture field displayed in Figure 5 is therefore reduced to the field $h_f(x,z)$ shown in Figure 8 (with the same color scale). As wee see, the middle channel remains, while high frequency variations are removed.

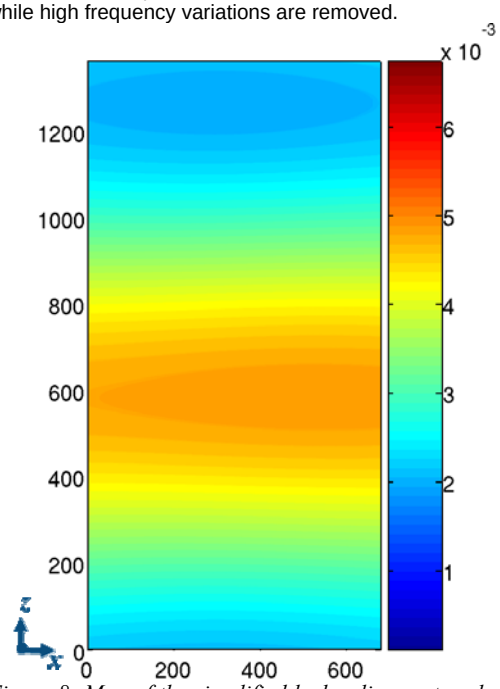

Figure 8: Map of the simplified hydraulic aperture h_f in m. Here, it is obtained by Filtering the previous hydraulic aperture: average and 1st Fourier modes along x and y are left. The spatial coordinates are in m.

Such low frequency variations might be obtained with field measurement. Let us assume that we only have this data to evaluate the heat exchange.

A quick and simple approximation of the thermal field is to use the exponential law with a local variable length of reference $R_f(x,y)$ which change accordingly to the local hydraulic aperture $h_f(x,z)$. $R_f(x,y$ is defined similarly to $R_{//}$ in Eq. 4 by putting $h_f(x,z)$ in place of A:

$$\overline{T}_f(x,y) = (T_0 - T_r)\exp\left(-\frac{x}{R_f(x,y)}\right) + T_r \quad \text{[Eq. 15]}$$

where $R_f(x,y) = -\frac{\Delta P}{l_x}\frac{[h_f(x,y)]^4}{24\eta Nu\,\chi}$ [eq. 16].

From this last expression, we obtain the thermal field shown in Figure 9. The main spatial channel of the complete thermal field (Figure 6) is still visible, and even if the fluid temperature evolves slightly differently (quicker), it may roughly give an idea of what thermically happens.

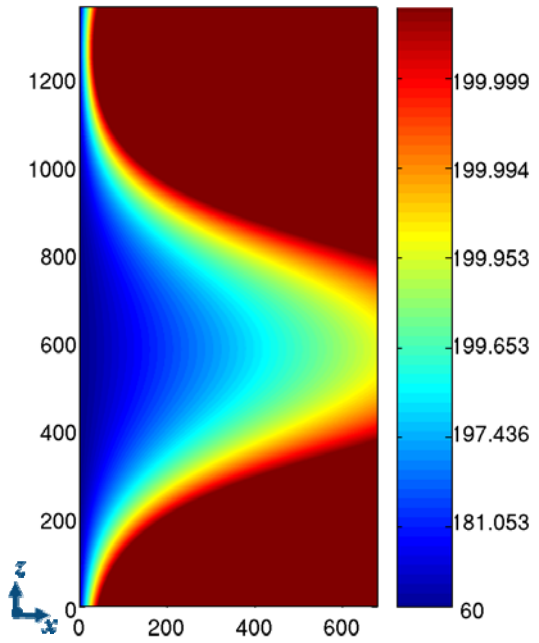

Figure 9: Map of the simplified temperature field $\overline{T}_f$ obtained using the previous filtered aperture (fig. 8) in the exponential law. Color scale is in °C and it changes exponentially.

CONCLUSION AND COMPLEMENT

We propose a numerical model to estimate the heat exchange at the fracture scale between cold fluid and hot surrounding rock. We supposed to be in permanent laminar regime and the numerical model is based on a lubrication approximation for the fluid flow (Reynolds equation). We introduce a “thermal lubrication” approximation which leads us to a quartic profile of the temperature across the aperture. It is obtained by assuming that in plane convection is dominant compared to in plane conduction (low in plane Peclet number). Moreover, due to the lubrication approximation, the out plane convection is neglected and the heat conduction initiated by the difference of temperature between rock and fluid is supposed to be the major out plane phenomenon.

Our model shows that the roughness of the fracture can be responsible for fluid channeling inside one single fracture. In this zone of high convection the heat exchange is inhibited: the fluid needs a longer distance to reach the rock temperature. Besides, the temperature evolution is inhomogeneous along the fracture height. We characterize it on average thanks to a thermal length and a thermal aperture which change according to the morphology.

In this proceeding, we only illustrate a case of rough aperture which leads to inhibited thermalization with a long channeling. With other apertures (not illustrated here) we observe that roughness may also locally highly reduce the convection (because of barriers of rock perpendicular to the main flow) which locally enhances the heat exchange (high conduction compared to convection).

In any case, we notice that the temperature distribution is strongly affected by the hydraulic flow.

By characterizing the hydraulic and thermal exchange with reduced parameters, we see that average value of the geometrical aperture provide too little information to characterize the fluid temperature. In contrast, the

knowledge of the main spatial variation of the hydraulic aperture (here observed by keeping only the very low spatial frequencies using Fourier filtering) brings interesting information about the spatial thermal field.
Moreover knowing the real distance covered by fluid particles may improve the temperature estimation. Indeed, it seems that the thermal field evolves exponentially along the trajectory lines. That brings back to the notion of tortuosity of the flow inside the fracture.
If the main variations of the geometrical field are known, it is also possible to compute the hydro-thermal fields in the same way as we have explained in the "Modeling" part. The main spatial hydro-thermal features can be obtained using apertures fields presenting various features (self affine or not). The macroscopic spatial correlation of the aperture is probably an important parameter ruling the hydro-thermal behavior.

We thank Albert Genter, Reinhard Jung Marion, Patrick Nami and Marion Schindler for discussion about this modeling.

REFERENCES

Bachler, D., Kohl, T., Rybach, L., (2003), Impact of grabenparallel faults on hydrothermal convection – rhine graben case study. *Phys. Chem. Earth,* **28**, 431-441.

Bataillé, A., Genthon, P., Rabinowicz, M. & Fritz, B. (2006), Modeling the coupling between free and forced convection in a vertical permeable slot: Implications for the heat production of an Enhanced Geothermal System, *Geothermics*, **35**, 654–682

Batchelor, G.K. (1967), An introduction to fluid dynamics, (*Cambridge University Press*, Cambridge)

Boffa, J.M., Allain C. & Hulin, J.P. (1998), Experimental analysis of fracture rugosity in granular and compact rocks. *Eur. Phys. J. Appl. Phys.,* **2**, 281-289.

Bouchaud, E. (1997), Scaling properties of cracks. *J. Phys. Cond. Matter,* **9**, 4319-4344

Brown, S. R. (1987), Fluid flow through rock joints : the effect of surface roughness. *J. Geophys. Res.,* **92**, 1337-1347

Brown, S.R. & Scholz, C.H. (1985), Broad bandwidth study of the topography of natural rock surfaces. *J. Geophys. Res.,* **90**, 12575-12582.

Cox, B. L. & Wang, J.S.Y. (1993), Fractal surfaces : measurement and application in earth sciences, *Fractal*, **1**, 87-115

Gentier, S., Rachez, X. Dezayes, C. Hosni, A., Blaisonneau, A, Genter, A. & Bruel, D. (2005), Thermohydro-mechanical modelling of the deep geothermal wells at Soultz-sous-Forêts. *Proceedings of EHDRA scientific conference.*

Gérard, A., Genter, A., Kohl, T., Lutz, P., Rose, P. & Rummel, F. (2006), The deep EGS (Enhanced geothermal System) project at Soultz-sous-Forêts (Alsace, France), *Geothermics*, **35**, 473-483

Heuer, N. Küpper, T. & Windelberg, D. (1991), Mathematical model of a Hot Dry Rock system, *Geophys. J. Int.,* **105**, 659-664

Iwai, K., (1976), Fundamental Studies of Fluid Flow Through a Single Fracture, Ph.D. Thesis, University of California, Berkeley.

Kolditz, O. & Clauser, C. (1998), Numerical simulation of flow and heat transfer in fractured cristalline rocks : application to the hot dry rock site in Rosemanowes (U.K.), *Geothermics,* **27** (1), 1-23

Landau, L. & Lifchitz, E. (1994), Physique théorique mécanique des fluides, 3è éd., p. 280

Méheust, Y. & Schmittbuhl, J. (2000) Flow enhancement of a rough fracture. *Geophys. Res. Lett.,* **27**, 2989-2992

Méheust Y. & Schmittbuhl, J. (2001), Geometrical heterogeneities and permeability anisotropy of rough fractures. *J. Geophys. Res.* **106**, 2089-2102

Méheust, Y. & Schmittbuhl, J. (2003), Scale effects related to flow in rough fractures. *PAGEOPH* **160 (5-6)**, 1023-1050

Méheust, Y. Ph.D. thesis, (2002), Ecoulements dans les fractures ouvertes, Université Paris Sud.

Neuman, S., (2005), Trends, prospects and challenges in quantifying flow and transport through fractured rocks. *Hydrogeol. J.*, **13**, 124-147.

Pinkus, O. & Sternlich, B. (1961), Theory of hydrodynamic Lubrication, Mc Graw-Hill, New York

Plouraboué, F., Roux, S. Schmittbuhl, J., Vilotte, J.P. (1995), Geometry of contact between self-affine surfaces, *Fractals*, **3** (1), 113-122

Plouraboué, F., Kurowski, P., Boffa, J.M., Hulin, J.P. & Roux, S. (2000), Experimental study of the transport properties of rough self-affine fractures, *J. of Contaminant Hydrology***, 46**, 295-318

Power, W. L., Tullis, T.E. Brown, S.R, Boitnott, G.N. & Scholz, C.H. (1987), Rhougness of natural fault surfaces, *Geophys. Res. Lett*., **14**, 29-32

Press, W. H., Teukolsky, S. A., Vetterling, W. T. & Flannery, B.P. (1992), Numerical Recipes (*Cambridge University Press*, New York)

Rachez, X., Gentier, S. & Blaisonneau, A. (2007), Current status of BRGM modeling activities at the Soultz EGS reservoir: hydro-mechanical modeling of the hydraulic stimulation tests and flow and transport modelling of the in-situ tracer test. *Proceedings of EHDRA scientific conference*

Roux, S., Schmittbuhl, J., Vilotte, J.P. & Hansen, A. (1993), Some physical properties of self-affine rough surfaces. *Europhys. Lett.,* **23**, 277-282.

Sanjuan, B., Pinault, J.L., Rose, P. Gerard, A., Brach, M., Braibant, G., Crouzet, C., Foucher, J.C., Gautier, A & Touzelet, S. (2006), Tracer testing of the geothermal heat exchanger at Soultz-sous-Forets (France) between 2000 and 2005, *Geothermics,* **35**, (5-6), 622-653

Santucci, S., Måløy, K.J., Delaplace, A., Mathiesen, J., Hansen, A., Haavig Bakke, J.Ø., Schmittbuhl, J., Vanel, L., & Ray, P. (2007), Statistics of fracture surfaces Physical Review E, **75** (1), 016104

Sausse, J., Dezayes, C., Genter, A. & Bisset, A. (2008), Characterization of fracture connectivity and fluid flow pathways derived from geological interpretation and 3D modelling of the deep seated EGS reservoir of Soultz (France). *Proceedings, thirty-Third workshop on Geothermal Reservoir Engineering, Stanford, California*.

Schmittbuhl, J., Gentier S. & Roux, S. (1993), Field measurements of the roughness of fault surfaces. *Geophys. Res. Lett.*, **20**, 639-641

Schmittbuhl, J. Schmitt, F & Scholz, C (1995), Scaling invariance of crack surfaces. *J. Geophys. Res.,* **100**, 5953-5973

Spurk, J. H. & Aksel, N. (2008), Fluid Mechanics, 2nd ed., (*Springer)*, p.516

Stokes, G.G. (1846), On the theories of the internal friction of fluids in motion, and of the equilibrium and motion of elastic solids. *Trans. Cambr. Phil. Soc,* **8**, 287-319

Taine J. & Petit, J.P. (2003), Transferts thermiques, 3rd ed., (*Dunod*), p.449

Turcotte, D. L. & Schubert, G. (2002) Geodynamics, 2nd ed. (*Cambridge University Press*), Chap. 6, p.262-264

Zimmerman, R. W., Kumar, S. & Bodvarsson, G. S. (1991) Lubrication Theory Analysis of Rough-Walled Fractures, *Int. J. Rock. Mech.,* **28**, 325-331.